

Second-Order Steady Forces on Multiple Cylinders in a Rectangular Periodic Array

by Masashi KASHIWAGI

Research Institute for Applied Mechanics, Kyushu University
6-1 Kasuga-koen, Kasuga-city, Fukuoka 816-8580, Japan

1. Introduction

Effects of hydrodynamic interactions among multiple cylinders must be expected not only on the first-order forces and wave-induced motions but also on higher-order hydrodynamic quantities. The present paper is concerned with the characteristics of second-order steady forces on each cylinder in a rectangular array composed of many identical cylinders with equal separation distance.

Recently, Kashiwagi (2000) presented an effective calculation method for the wave drift force on the basis of the momentum conservation principle. However, this method (referred to as the far-field method) gives only the total forces in the horizontal plane and the yaw moment on the whole structure.

Meanwhile, the wave drift force can also be computed by integrating the pressure over the wetted surface of a structure, which enables us to evaluate the local forces on each cylinder. Based on this direct pressure-integration method, an accurate numerical calculation method is presented in this paper. Validity and numerical accuracy of the method are confirmed by comparison with the results of the far-field method and experimental results measured using 64 truncated circular cylinders arranged in 4 rows and 16 columns.

2. Formulation and Second-Order Forces

A column-supported large floating structure is considered, which comprises a thin upper deck and a large number of identical and equally-spaced buoyancy columns. The elementary column considered here is a truncated circular cylinder with radius a and draft d . The distance between centerlines of adjacent cylinders is $2s$ in both x - and y -axes of a Cartesian coordinate system. The positive z -axis is directed downward, with $z = 0$ the undisturbed free surface and $z = h$ the constant water depth.

The structure is allowed to move with unsteady motions of six degrees of freedom in response to the wave excitation. The vectors of the translational and rotational motions are denoted by $\boldsymbol{\xi}(t)$ and $\boldsymbol{\alpha}(t)$, respectively; the magnitudes of which are assumed to be small. Under the usual potential-flow assumptions, we introduce the velocity potential, Φ , with which the hydrodynamic pressure can be computed from Bernoulli's equation. Then the wave force on a body can be obtained by integrating the pressure multiplied by the unit normal vector over the instantaneous body's wetted surface, say $S(t)$.

Assuming weak nonlinearities, the velocity potential and the motion vectors can be written as a perturbation series in a small parameter which is usually taken as the wave slope. Furthermore, using Taylor's expansion for the pressure and unit normal vector on $S(t)$ with respect to the mean body surface, S_B , the wave forces on a body can be expressed also in a perturbation series. Skipping details of the derivation (see Ogilvie (1983) for example), the calculation formulae for the first-order and second-order forces can be summarized as follows:

$$\mathbf{F}^{(1)} = \rho \iint_{S_B} \frac{\partial \Phi^{(1)}}{\partial t} \mathbf{n} dS - \rho g \iint_{S_B} \Xi_3^{(1)} n_3 \mathbf{k} dS, \quad (1)$$

$$\mathbf{F}^{(2)} = \rho \iint_{S_B} \frac{\partial \Phi^{(2)}}{\partial t} \mathbf{n} dS - \rho g \iint_{S_B} \Xi_3^{(2)} n_3 \mathbf{k} dS + \mathbf{F}_q^{(2)}, \quad (2)$$

where

$$\begin{aligned} \mathbf{F}_q^{(2)} = & \frac{1}{2} \rho \iint_{S_B} |\nabla \Phi^{(1)}|^2 \mathbf{n} dS - \frac{1}{2} \rho g \oint_{C_B} \{\zeta_R^{(1)}\}^2 \mathbf{n} dl \\ & + \rho \iint_{S_B} \boldsymbol{\Xi}^{(1)} \cdot \nabla \left(\frac{\partial \Phi^{(1)}}{\partial t} \right) \mathbf{n} dS + \boldsymbol{\alpha}^{(1)} \times \mathbf{F}^{(1)} \\ & - \rho g \iint_{S_B} \alpha_3^{(1)} (\alpha_1^{(1)} x + \alpha_2^{(1)} y) n_3 \mathbf{k} dS. \end{aligned} \quad (3)$$

Here $\zeta_R^{(1)}$ in (3) denotes the first-order relative wave elevation given by

$$\zeta_R^{(1)} = \frac{1}{g} \frac{\partial \Phi^{(1)}}{\partial t} \Big|_{z=0} - \Xi_3^{(1)}, \quad (4)$$

which must be evaluated along the mean waterline C_B ; ρ is the fluid density; g is the gravitational acceleration; \mathbf{n} is the unit normal vector directing into the fluid from the mean body surface S_B ; $\Xi^{(1)} = \xi^{(1)} + \alpha^{(1)} \times \mathbf{r}$ and thus $\Xi_3^{(1)} = \xi_3^{(1)} + \alpha_1^{(1)}y - \alpha_2^{(1)}x$; \mathbf{k} is the unit vector in the z -direction of the space-fixed coordinate axes. The corresponding expressions for the moment can be obtained in a similar form.

The present paper is concerned with the second-order steady forces, which can be computed by taking time-average over one period of $\mathbf{F}_q^{(2)}$ which contains only quadratic products of first-order quantities.

3. Solution of First-Order Problem

The first-order quantities are assumed to be time-harmonic with circular frequency of the incident wave, ω , and are expressed as

$$\Phi^{(1)} = \text{Re} \left[\frac{gA}{i\omega} \left\{ \phi_I + \phi_S - K \sum_{k=1}^6 X_k (\phi_k + \varphi_k) \right\} e^{i\omega t} \right], \quad (5)$$

$$\xi_k^{(1)} = \text{Re} \left[A X_k e^{i\omega t} \right], \quad \alpha_k^{(1)} = \text{Re} \left[\frac{A}{a} X_{k+3} e^{i\omega t} \right], \quad (6)$$

where A is the amplitude of the incident wave, $K = \omega^2 a/g$ is the nondimensional wavenumber, and X_j ($j = 1 \sim 6$) is the complex motion amplitude expressed in a nondimensional form.

ϕ_I and ϕ_S are the incident-wave and scattering potentials, respectively, and the sum, $\phi_I + \phi_S \equiv \phi_D$, is referred to as the diffraction potential. For plane waves propagating in the direction with angle β relative to the positive x -axis, ϕ_I is given by

$$\phi_I = \frac{\cosh k_0(z-h)}{\cosh k_0 h} e^{-ik_0(x \cos \beta + y \sin \beta)}, \quad (7)$$

where k_0 is the solution of the wave dispersion relation, $k_0 \tanh k_0 h = K$.

In the radiation problem, ϕ_k in (5) denotes the velocity potential of a single body oscillating in the k -th mode (with no interactions), and φ_k represents the remaining part due to hydrodynamic interactions with radiated and scattered waves by the other bodies, which are essentially the same as the scattering problem.

Therefore the boundary conditions to be satisfied on the body surface, S_B , are given as

$$\frac{\partial \phi_D}{\partial n} = 0, \quad \frac{\partial \phi_k}{\partial n} = n_k, \quad \frac{\partial \varphi_k}{\partial n} = 0, \quad (k = 1 \sim 6) \quad \text{on } S_B \quad (8)$$

where $\mathbf{n} = (n_1, n_2, n_3)$ and $\mathbf{r} \times \mathbf{n} = (n_4, n_5, n_6)$.

Solutions satisfying (8) and other free-surface and radiation conditions may be obtained by Kagemoto & Yue's interaction theory (1986). The expressions of the velocity potentials appropriate near the j -th body can be summarized as follows:

$$\phi_D^j = \phi_I + \{A_S^j\}^T \{\psi_S^j\}, \quad (9)$$

$$\phi_k^j = \{\mathcal{R}_k^j\}^T \{\psi_S^j\}, \quad \varphi_k = \{A_k^j\}^T \{\psi_S^j\}, \quad (10)$$

where $\{A_S^j\}$ in (9) and $\{A_k^j\}$ in (10) are unknown coefficient vectors of scattered waves to be determined, and $\{\psi_S^j\}$ is the vector comprised of the progressive and evanescent wave components, which are expressed as

$$\{\psi_S^j\} = \left\{ \begin{array}{l} \frac{\cosh k_0(z-h)}{\cosh k_0 h} H_m^{(2)}(k_0 r_j) e^{-im\theta_j} \\ \frac{\cos k_n(z-h)}{\cos k_n h} K_m(k_n r_j) e^{-im\theta_j} \end{array} \right\}. \quad (11)$$

Here k_n ($n = 1, 2, \dots$) denotes the evanescent-mode wavenumbers satisfying $k_n \tan k_n h = -K$. The local cylindrical coordinate system (r_j, θ_j, z) has been used, with the origin placed at the center of the j -th body. The number of Fourier series in the θ -direction, m , is taken as $0, \pm 1, \pm 2, \dots$.

Once the velocity potentials are determined, it is straightforward to compute the first-order forces, $\mathbf{F}^{(1)}$ defined by (1), on each of the cylinders in the array. The complex amplitude X_k defined in (6) will be determined by solving the motion equations of the structure consisting of many buoyancy cylinders.

4. Outline of Numerical Computations

As the first step of numerical computations, the first-order boundary-value problems for a single cylinder were solved by the boundary element method using 9-point quadratic representations for the surface geometry and velocity potential.

In computing the wave interactions by Kagemoto & Yue's theory, the number of Fourier series in the θ -direction (M) and of evanescent wave modes (N) were determined to be $M = 5$ and $N = 3$ after a convergence check. In this case, the total unknowns for $N_B = 64$ cylinders are $(2M + 1) \times (N + 1) \times N_B = 2816$. To enhance numerical efficiency, the double symmetry relations with respect to the x - and y -axes were exploited, reducing the number of unknowns to $1/4$ (i.e. $2816/4 = 704$).

In computing the second-order steady forces, the spatial derivatives of the velocity potential over the submerged surface, S_B , and the line integral along the waterline, C_B , were evaluated using the boundary condition (8) and quadratic isoparametric representations for the velocity potential and coordinates (x, y, z) .

5. Outline of Experiments

A truncated circular cylinder with diameter $D (= 2a) = 114$ mm was used as an elementary float, and 64 cylinders were arranged in a rectangular array with 4 rows (in the y -axis) and 16 columns (in the x -axis) with equal separation distance of $2s = 2D$ between the centerlines of adjacent cylinders in both x - and y -axes. The draft of cylinders was set to $d = D$ and $2D$, but the results of $d = 2D$ will be mainly shown because there were no essential differences.

Although the effects of wave-induced motions can be taken into account in the calculation method, the motions of the structure were completely fixed, and the experiments were carried out in head waves ($\beta = 0^\circ$). The wave forces were measured by dynamometers at 6 different positions; No. 1, No. 9, and No. 15 Columns. (16 columns are numbered from the upwave side.) By symmetry in head waves, the lines at $y = \pm D$ are called the inside and the lines at $y = \pm 3D$ are called the outside. Then the positions of measured cylinders are distinguished with the column number and the inside or outside line. The frequency range in the measurements was $Ks (= \omega^2 s/g) = 0.2 \sim 1.6$ and the wave steepness H/λ (the ratio of wave height to wave length) was set to approximately $1/50$.

6. Results and Discussion

Numerical accuracy of the present method was checked by comparing the sum of the local steady forces on 64 cylinders with independent results by the far-field method developed by Kashiwagi (2000). Some results are shown in Table 1 for the case of $\beta = 30^\circ$, $s = D$, $d = 2D$, and $h = 7.5d$. In computing the wave-induced motions, the center of gravity was assumed to be on the water plane, and the radii of gyration in roll, pitch, and yaw modes were set to $0.25B$, $0.25L$, and $0.25L$, respectively, with B and L being the breadth and length of the structure.

Table 1 Steady forces in surge, sway, and yaw on a structure with 64 circular cylinders arranged periodically in the array of 4 rows and 16 columns, computed by the far-field method and the pressure integration method. ($d = 2D$, $s = D$, $h = 7.5d$, $\beta = 30^\circ$)

| <i>By Far-Field Method (Momentum-Conservation Principle)</i> | | | | | | |
|--|---------------------|---------|----------|--------------------------|---------|----------|
| Ks | Diffraction Problem | | | Including Motion Effects | | |
| | FX | FY | MZ | FX | FY | MZ |
| 0.50 | 0.05413 | 0.00876 | 0.00412 | 0.14638 | 0.01407 | -0.10189 |
| 1.00 | 0.08821 | 0.04253 | 0.02977 | 0.08946 | 0.04258 | 0.03098 |
| 1.50 | 1.6217 | 0.08032 | -0.00668 | 1.6218 | 0.08030 | -0.00606 |
| 1.75 | 3.9364 | 0.27782 | 0.40703 | 3.9369 | 0.27766 | 0.40795 |
| 2.00 | 3.2052 | 0.70410 | -0.26574 | 3.2048 | 0.70387 | -0.26517 |
| 2.50 | 0.98615 | 0.50644 | -0.37112 | 0.98633 | 0.50677 | -0.37146 |
| <i>By Near-Field Method (Direct Pressure Integration)</i> | | | | | | |
| Ks | Diffraction Problem | | | Including Motion Effects | | |
| | FX | FY | MZ | FX | FY | MZ |
| 0.50 | 0.05576 | 0.00874 | 0.00343 | 0.17035 | 0.01336 | -0.10203 |
| 1.00 | 0.08868 | 0.04209 | 0.02975 | 0.08997 | 0.04213 | 0.03099 |
| 1.50 | 1.6222 | 0.08027 | -0.00664 | 1.6223 | 0.08025 | -0.00602 |
| 1.75 | 3.9368 | 0.27791 | 0.40708 | 3.9373 | 0.27775 | 0.40799 |
| 2.00 | 3.2056 | 0.70419 | -0.26571 | 3.2052 | 0.70396 | -0.26513 |
| 2.50 | 0.98646 | 0.50627 | -0.37130 | 0.98664 | 0.50661 | -0.37164 |

We can see from Table 1 that very good agreement exists between the far-field method and the present pressure-integration method. For higher frequencies, the steady surge (FX) and sway (FY) forces and steady yaw moment (MZ) were dominated by the diffraction component, because the structure considered here is large in size compared to the wavelength of the incident wave and thus the wave-induced motions are relatively small.

Computed local steady forces acting on elementary cylinders are shown from Fig. 1 through Fig. 6 together with measured results. From these figures we can observe the followings:

- 1) At the upwave side (Column No. 1), variation of the steady force is rapid in the frequency range lower than the near trapped-mode frequency ($Ks \simeq 1.24$ in the present case), but this variation becomes mild as the position of the cylinder concerned goes downstream.
- 2) For frequencies higher than $Ks = 1.24$, the local steady forces on upwave cylinders become positive and large, dominating the total drift force on the structure.
- 3) The steady force on a cylinder along the inside line in the array is larger than that on a cylinder along the outside line in the variation amplitude with respect to the frequency.
- 4) Computed results by the present method are in good agreement with measured results, except for the very narrow frequency range just below the near trapped-mode frequency.

References

- [1] Kashiwagi, M. (2000): "Wave Drift Force and Moment on a VLFS Supported by a Great Number of Floating Columns", *Proc. 10th International Offshore and Polar Engineering Conf.*, Seattle, Vol. 1, pp. 49–56
- [2] Ogilvie, T.F. (1983): "Second Order Hydrodynamic Effects on Ocean Platforms", *International Workshop on Ship and Platform Motion*, Berkeley, pp. 205–265
- [3] Kagemoto, H. and Yue, D.K.P. (1986): "Interactions among Multiple Three-Dimensional Bodies in Water Waves: An Exact Algebraic Method", *Journal of Fluid Mechanics*, Vol. 166, pp. 189–209

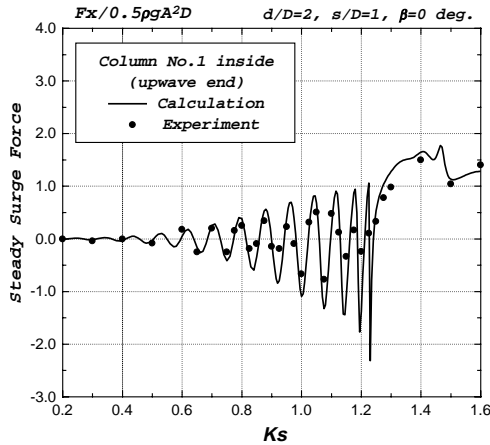


Fig. 1 Steady surge force on the cylinder at Column No. 1 along the inside line

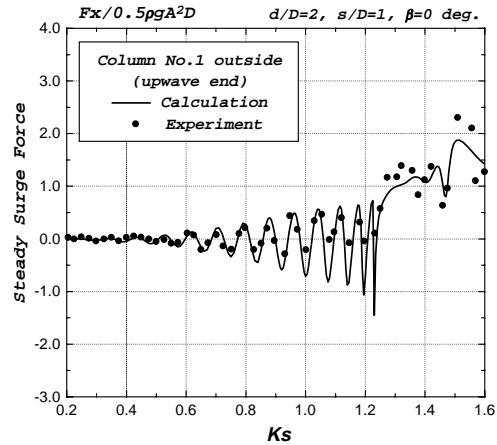


Fig. 2 Steady surge force on the cylinder at Column No. 1 along the outside line

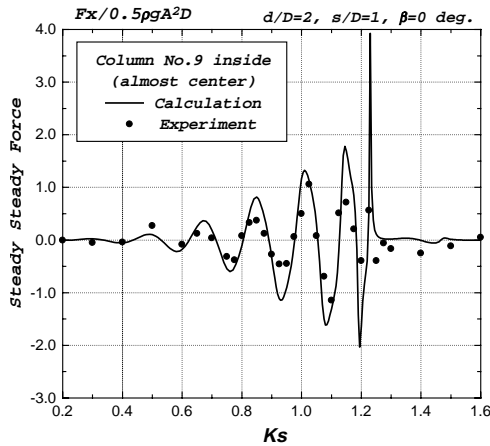


Fig. 3 Steady surge force on the cylinder at Column No. 9 along the inside line

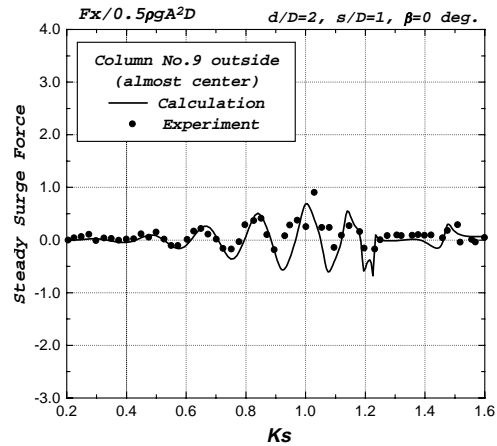


Fig. 4 Steady surge force on the cylinder at Column No. 9 along the outside line

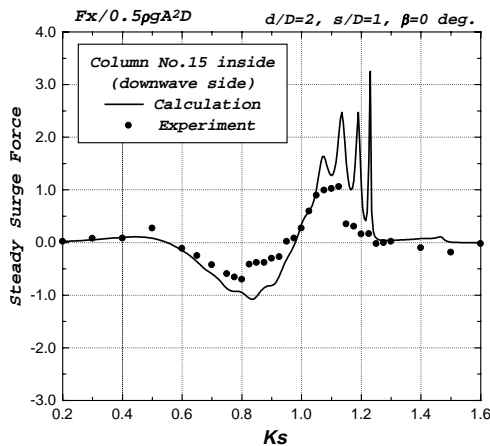


Fig. 5 Steady surge force on the cylinder at Column No. 15 along the inside line

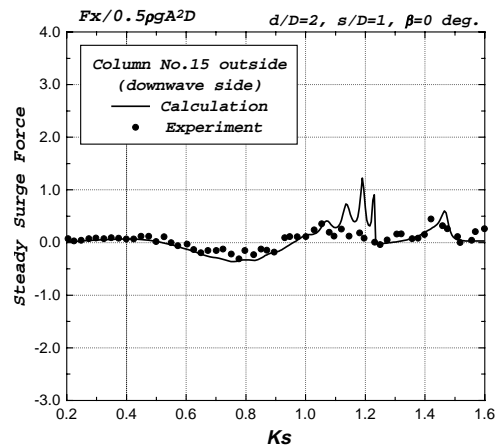


Fig. 6 Steady surge force on the cylinder at Column No. 15 along the outside line